

Synthesis and characterization of water-soluble ZnO quantum dots prepared through PEG-siloxane coating

Ralph-Olivier Moussodia,^a Lavinia Balan^b and Raphaël Schneider^{*a}

Received (in Montpellier, France) 21st December 2007, Accepted 20th February 2008

First published as an Advance Article on the web 27th March 2008

DOI: 10.1039/b719642c

A new method for the synthesis of biocompatible and multifunctional semiconductor ZnO quantum dots (QDs) through reaction of oleate-capped ZnO QDs with a poly(ethylene glycol)-siloxane is reported. The size, shape, crystal structure and the optical properties of water-soluble ZnO QDs were characterized by atomic force microscopy (AFM) and by their absorption and photoluminescence (PL) spectra. The results showed that well-dispersed ZnO QDs with *ca.* 6.0 nm in diameter were obtained after surface modification. Fluorescence spectra indicated that the QDs exhibited good fluorescence features after coating.

Introduction

Semiconductor (quantum dots, QDs) and metallic nanoparticles have attracted a tremendous interest in the past two decades due to their unique optical and electronic properties. This interest is motivated by the nanoparticles' remarkable photochemical stability and several properties, including (i) size-dependent broad emission, (ii) very high extinction coefficient, (iii) readily size-tunable narrow emission, and (iv) high fluorescence quantum yields.^{1–4} In addition, QDs are much more stable to the permanent loss of fluorescence than conventional organic fluorophores.^{5,6} All these features offer several advantages for applications in advanced biosensors, bioanalytical assays, cell imaging, and *in vivo* animal targeting.

Compared to II–VI semiconductor compounds, such as CdTe or CdSe, ZnO has a wide band-gap (3.37 eV) and rather large exciton binding energy (60 meV), which makes the exciton stable even at room temperature. ZnO is an extremely important material for applications such as gas sensors,⁷ optoelectronics,⁸ field-emission devices,⁹ photo-anodes or dye-sensitized solar cells,¹⁰ and bio-imaging.¹¹ Furthermore, compared to Cd-containing QDs which release Cd²⁺ ions under oxidizing or long UV radiations conditions,¹² ZnO is an environmentally friendly material, which is desirable for bio-applications such as cancer detection.¹³

During the past years, steady progress has been made to obtain nearly monodispersed ZnO nanoparticles simply by hydrolysing zinc acetate in alcohol solutions.¹⁴ Size, shape and luminescent properties could be readily controlled by capping the QDs with dodecylamine (DDA), trioctylphosphine oxide (TOPO), dodecanethiol, oleic acid, alkoxysilanes or SiO₂.^{11,15–18} These nanoparticles are generally soluble in organic solvents, such as toluene, hexane or chloroform.

However, a water soluble surface is necessary for biological labels. ZnO nanoparticles are not stable in water. This instability is related to their surface luminescent mechanisms. Water molecules are able to attack the luminescent centers on the ZnO surface and destroy them rapidly. Several strategies have been developed to transfer ZnO nanocrystals in water. Basic hydrolysis of hydrophilic poly(ethylene glycol)zinc carboxylates yielded stable polymer-grafted ZnO nanoparticles dispersible in ethanol but neither solubility nor stability of these colloids in water was reported.^{19,20} Nanocomposites prepared from ZnO nanoparticles, 3-(trimethoxysilyl)propyl methacrylate and the hydrophilic monomer 2-hydroxyethyl methacrylate have also been described. The large aggregates obtained after polymerization were not soluble in water.²¹ Jana *et al.* reported the preparation of ZnO nanoparticles capped with 3-aminopropyltrimethoxysilane (APTMS) which were soluble in water.²² The amine group of the ligand contributes however to the stability of these QDs due to the strong affinity of nitrogen towards Zn atoms at the surface of the nanoparticles. Finally, Xiong *et al.* have recently reported the first example of ZnO-polymer core-shell nanoparticles which are stable in water even in the presence of strong acids or alkalis. However, the microspheres obtained have diameters ranging from 150 to 450 nm, and are therefore too large to enter into cells by an endocytotic mechanism.²³

In this article, we intend to modify the ZnO nanoparticle surfaces to promote the stability of colloid suspensions in water thus preserving the luminescent properties of the nanoparticles. Silanization is a ligand-exchange method that has recently been used with success to transfer hydrophobic nanoparticles in water.^{24,25} We report here the use of a poly(ethylene glycol) (PEG)-siloxane covalently linked to the surface of ZnO QDs to make these nanoparticles water-dispersible. The obtained ZnO nanocrystals were characterized by atomic force microscopy (AFM), by UV-Vis absorption spectroscopy and by their photoluminescence properties. PEG-siloxane capped ZnO QDs were in the size range of 4–10 nm and no agglomeration was observed when these nanoparticles were stored at ambient conditions for several weeks in water. Finally, to provide a side group on the surface of the

^a Laboratoire de Chimie Physique et de Microbiologie pour l'Environnement, Nancy Université, CNRS, 29-30 rue Lionnois, F-54001 Nancy, France. E-mail: Raphael.Schneider@pharma.uhp-nancy.fr; Fax: +33 3 83 68 21 54; Tel: +33 3 83 68 21 56

^b Département de Photochimie Générale, CNRS-UMR 75253 rue Alfred Werner, Ecole Nationale Supérieure de Chimie de Mulhouse, Université de Haute-Alsace, 68093 Mulhouse, France

QDs that can be further conjugated to biomolecules or specially engineered domains, silanization was also performed with a PEG-siloxane and 3-aminopropyltrimethoxysilane (APTES).

Experimental

General experimental

Zinc acetate, oleic acid, tetraethylene glycol, tetramethylammonium hydroxide, triethoxysilane, allyl bromide, ethyl bromide, hydrogen hexachloroplatinate and 3-aminopropyltriethoxysilane were purchased from Aldrich and used without further purification. Ethanol and toluene were distilled before use. Ultrapure water was used as a solvent. All reactions were conducted in a three-neck flask under flowing nitrogen gas. 2-[Ethoxy(polyethyleneglycol)propyl]triethoxysilane **1** was prepared in three steps from tetraethylene glycol according to the procedure described by Yang *et al.* (Scheme 1).²⁶

To determine the morphology of the nanoparticles, the samples were analyzed *ex situ* by atomic force microscopy. AFM is an effective method for providing exact information about particle size and shape. Characterization was carried out using a Digital Instruments Nanoscope III. AFM measurements were done by contact mode using a Si₃N₄ tip with resonance frequency and spring constant being 100 kHz and 0.6 N m⁻¹, respectively to provide surface topography.

All the optical measurements were performed at room temperature (20 ± 2 °C) under ambient conditions. UV-Vis spectra were recorded on a Beckman DU 640 spectrometer. A FluoMax 2 Luminescence Spectrometer was used for the photoluminescence (PL) measurements. PL spectra were spectrally corrected and quantum yields were determined relative to quinine bisulfate in 0.05 M sulfuric acid ($\Phi = 0.55$).²⁷

Synthesis of oleate-capped ZnO QDs

Zinc acetate (220 mg, 1.2 mmol) was dissolved in hot ethanol (20 mL) under vigorous stirring. Oleic acid (70 μ L, 0.22 mmol) was then added and the mixture heated to reflux. In a separate flask, tetramethylammonium hydroxide (360 mg, 1.99 mmol) was dissolved in refluxing ethanol (5 mL). This solution was then rapidly injected in the flask containing Zn(OAc)₂ and oleic acid and the mixture was refluxed for 2 min. The mixture is then diluted with EtOH (50 mL) and cooled to 0 °C with an

ice-bath. A white precipitate of ZnO nanoparticles appeared. Particles were centrifuged (15 min at 4000 rpm) with removal of the supernatant. The resulting oleate capped ZnO QDs were washed several times with ethanol, in which they are insoluble, and finally suspended in toluene (10 mL). Oleate capped ZnO QDs were stored at 4 °C in the dark.

Water-solubilization of ZnO QDs

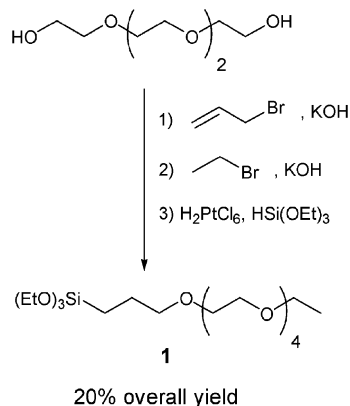
Cap exchange with PEG-siloxane **1** was used to replace the oleate ligands with a water-soluble layer, which allowed the QDs to be suspended in aqueous solution. Briefly, to the ZnO QDs in toluene previously prepared were added 1 mL of a 0.1 M of a solution of PEG-siloxane **1** in toluene and 1 mL of a 0.1 M TMAH solution in ethanol. The mixture was heated at 85 °C for 15 min. After cooling to room temperature and centrifugation (15 min at 4000 rpm), the nanoparticles were washed three times with toluene to remove the oleate ligand. Nanoparticles were redispersed in toluene (10 mL) and 1 mL of a 0.1 M TMAH solution were added. The mixture was heated at 85 °C for 30 min. After cooling, PEG-siloxane ZnO nanoparticles were separated by centrifugation, washed three times with toluene and finally dried *in vacuo* at room temperature for 15 h. PEG-siloxane capped ZnO QDs were redispersed in ultrapure water for further characterization.

Results and discussion

ZnO nanoparticles were prepared by hydrolyzing zinc acetate with tetramethylammonium hydroxide (TMAH) in ethanol.²² Oleic acid was used as a capping agent to control the particle growth. In order to directly observe the QDs formation and distribution, AFM images were obtained as shown in Fig. 1. AFM amplitude scans revealed discrete spherical entities with smooth and uniform surface features. The histogram of the island heights corresponding to the AFM image cross-section height analysis of these entities showed spherical-shaped particles with diameters ranging from 2.0 to 8.0 nm. Their average diameter determined from AFM was found to be 5.1 nm. Fig. 2 shows the absorption and the room-temperature photoluminescence (PL) of these QDs. A faint excitonic absorption peak at *ca.* 350 nm (3.54 eV) can be observed in the absorption spectrum due to the moderate size distribution of ZnO QDs. The observed ground-state exciton energy is slightly enhanced compared to the free exciton energy in the bulk (3.37 eV) due to the quantum-confinement effect.

In the PL spectrum shown in Fig. 2, a strong and broad peak is located at 545 nm. The wide emission lines were consistent with the broad size distribution of the nanocrystals, as demonstrated by the AFM image in Fig. 1. The full width at half maximum (FWHM) of the PL peak is *ca.* 135 nm. The PL quantum yield (QY) measured using quinine bisulfate as reference²⁷ was about 18%. This green-emission is commonly referred to as a deep-level or trap-state emission.^{28,29} More specifically, the green-emission is related to a singly ionized oxygen vacancy in ZnO and it results from radiative recombination of a photogenerated hole with an electron occupying the oxygen vacancy.³⁰

Surface functionalization of oleate-capped ZnO QDs was undertaken to improve their stability, to make them



Scheme 1 Synthesis of PEG-siloxane **1**.

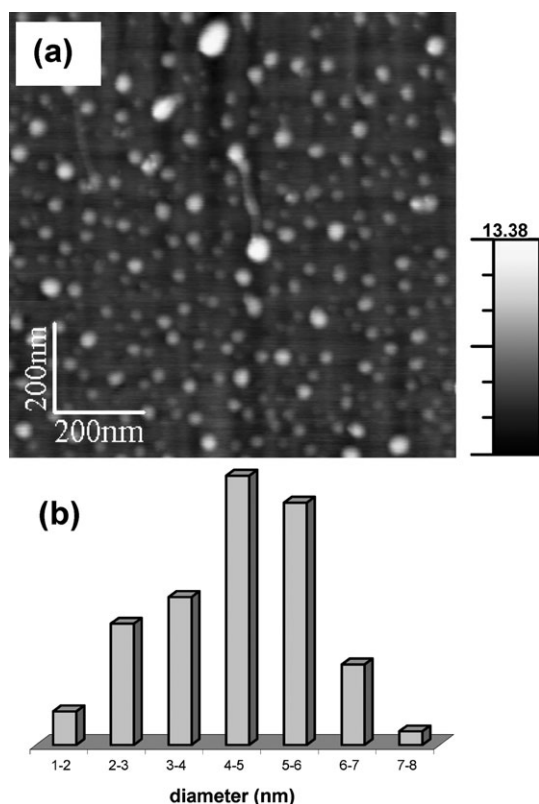


Fig. 1 (a) Atomic force microscopy (AFM) of oleate-capped ZnO nanoparticles deposited on a silicon wafer, and (b) particle size distribution determined using AFM heights.

biocompatible, and to strengthen their resistance to environmental changes. A $\text{Zn}(\text{OH})_2$ shell coating the ZnO surface was used for the modification of ZnO nanoparticles.³¹ The hydrophilic PEG-siloxane **1**, prepared in three steps for tetraethylene glycol,²⁴ was used for the coating to render the nanocrystals water-soluble. Functionalization was carried out using a two-stage silanization procedure initiated by TMAH as described in Scheme 2.²² To the oleate-capped ZnO QDs in toluene were added PEG-siloxane **1** and 1.0 eq. of TMAH. To avoid self-nucleation of the siloxane, its concentration was kept below 0.1 M. After heating for 15 min at 85 °C, ZnO particles functionalized with **1** were centrifuged to produce a pellet of QDs which was not soluble in toluene. The supernatant, free of QDs, was discarded and the precipitate treated again with

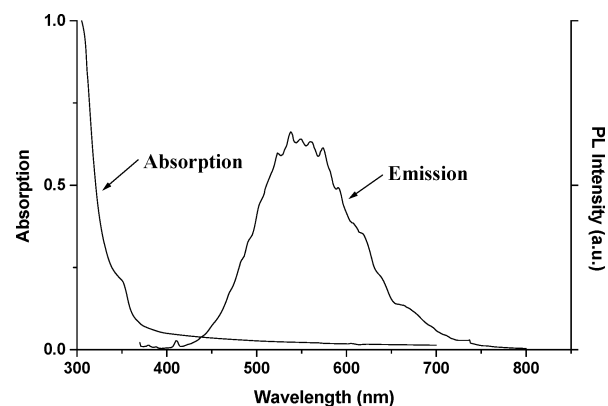
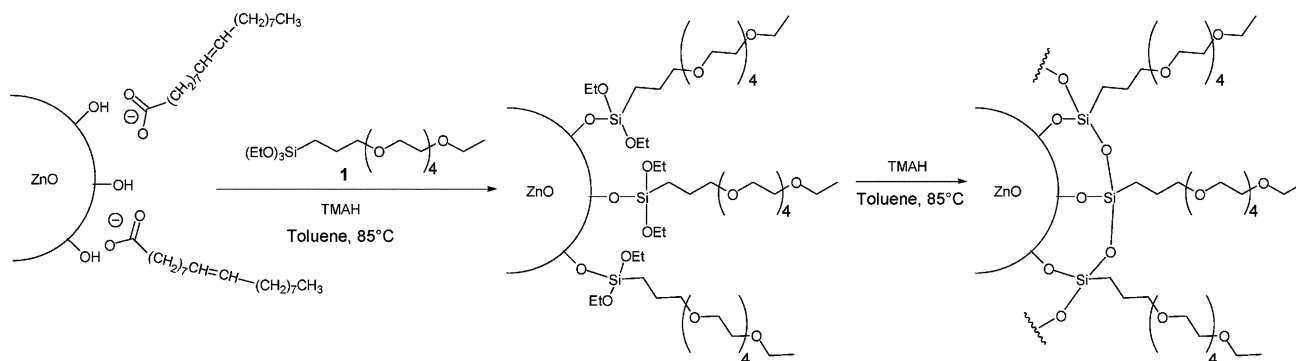


Fig. 2 Absorption and emission spectra of oleate-capped ZnO nanoparticles in toluene.

TMAH for the cross-linking of the PEG-siloxane at the surface of the QDs. No obvious aggregates of QDs or silica nanoparticles were observed using this procedure. After centrifugation and purification, ZnO capped with **1** could be redispersed in water, phosphate buffered saline (PBS) or ethanol, providing a clear homogeneous dispersion of nanocrystals.

It is well-known that the band gap of semiconductor nanocrystals increases with decreasing particle size due to quantum confinement effects. So the synthesis was first monitored by AFM to survey the change in nanocrystal size. Fig. 3 shows the overview image of the nanocrystals after functionalization with PEG-siloxane **1**. Well-dispersed and spherical-shaped nanodots can be observed. However, the AFM image and the corresponding size distribution indicate that the nanocrystals are more polydisperse than the starting oleate-capped QDs. Their average diameter is estimated to be 5.9 nm.

The re-dispersed water colloids have almost the same PL and UV-Vis absorption spectra as the oleate-capped ZnO QDs (Fig. 4). No significant shift was observed for the excitonic peak (*ca.* 350 nm) and for the green emission (*ca.* 540 nm) in comparison to the oleate-capped ZnO QDs (Fig. 2) confirming that aggregation did not occur during ligand exchange. However, the PL QY shows a significant change upon surface ligand exchange (PL QY is *ca.* 8% in water for ZnO capped with **1** relative to 18% for oleate-capped QDs). This decrease of the quantum yield could be related to variations of the thickness of the $\text{Zn}(\text{OH})_2$ shell during functionalization which



Scheme 2 Water-solubilization of ZnO nanoparticles.

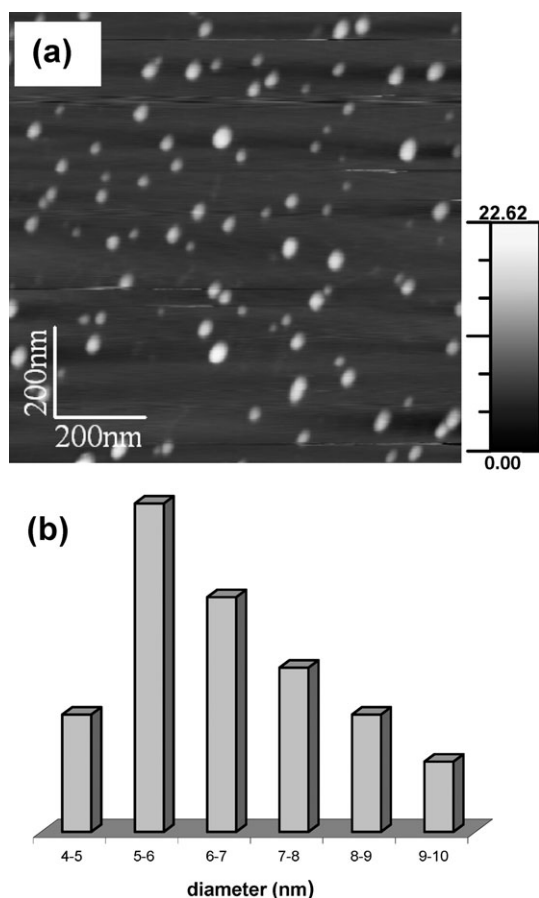


Fig. 3 (a) AFM of PEG-siloxane **1** capped ZnO nanoparticles, and (b) the particle size distribution determined using AFM heights.

are directly correlated with green trap emission intensities.¹⁵ ZnO colloids containing 1 or 10 mg of **1**-capped ZnO nanoparticles in 1 mL PBS were used to evaluate the stability of the QDs in aqueous solution. The UV-Vis and PL spectra (absorption and emission peak intensity and position vs. storage) of these samples were monitored over 10 days. Results obtained show that PL intensity and position (shift from 537 to 540 nm) remains almost unchanged over the 10 days indicating that the particles did not nucleate and grow when protected with PEG-siloxane **1**. Moreover, **1**-capped ZnO QDs did not undergo Ostwald ripening³² upon aging (over three months) either in the solvent-free state or in water.

ZnO QDs with mixed functional groups could also be synthesized using the same strategy. Siloxane-coating of the native oleate-capped ZnO QDs was undertaken with a mixture of **1** and 3-aminopropyltriethoxysilane (APTES) used in a 4 : 1 molar ratio. As shown in Fig. 5 and 6, well-dispersed nanoparticles with an average diameter of 6.4 nm and emitting from *ca.* 430 and 670 nm (QY = 8% in water) were produced. The amine group at the periphery of these QDs can be used for the covalent attachment of biomolecules allowing ZnO nanoparticles to be used as fluorescent labels for ultrasensitive detection and imaging.

Fig. 7 shows a photograph of a toluene/water biphasic mixture excited by an ultraviolet lamp containing (a) the starting hydrophobic oleate-capped QDs in toluene, and (b) the ZnO QDs dispersed in the aqueous phase after ligand

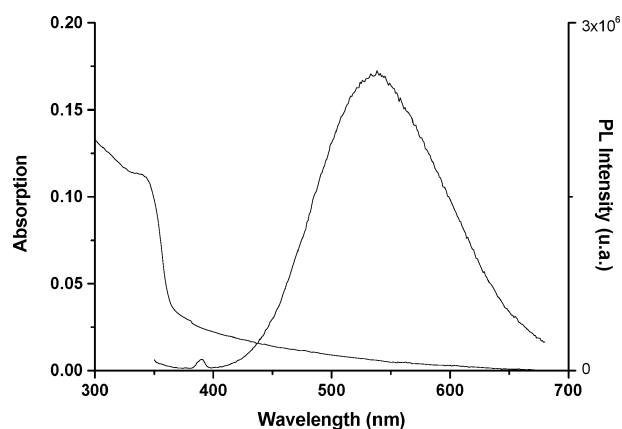


Fig. 4 Absorption and emission spectra of PEG-siloxane **1** capped ZnO nanoparticles in water.

exchange with **1** and APTES. The photoluminescence of the QDs was retained in water.

The effective mass model developed by Brus³³ was finally used to determine the variations of particles diameters in the course of their functionalization with siloxanes **1** and **1** + APTES. Indeed, the average particle diameter can approximately be calculated from the absorption onset using eqn (1) (the polarization term included in this model was neglected):

$$E_g = E_g^{\text{bulk}} + \frac{\hbar^2 \pi^2}{2er^2} \left(\frac{1}{m_e} + \frac{1}{m_h} \right) \quad (1)$$

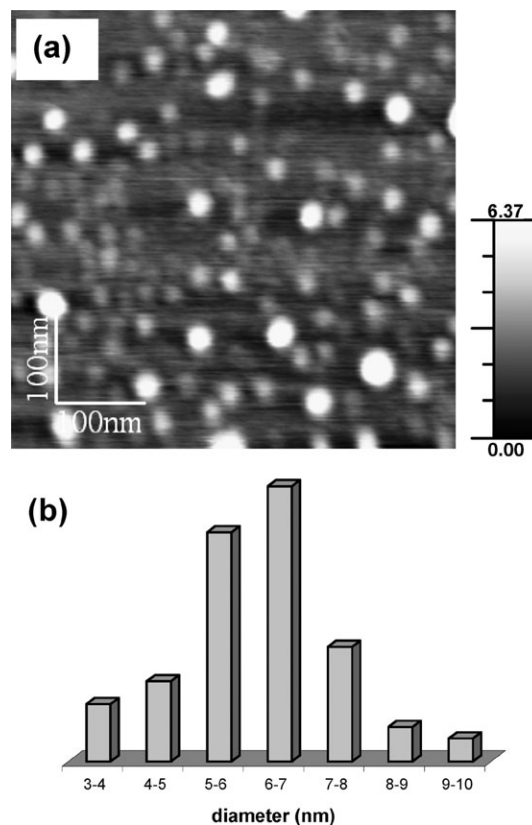


Fig. 5 (a) AFM of ZnO nanoparticles capped with PEG-siloxane **1** and APTES, and (b) the particle size distribution determined using AFM heights.

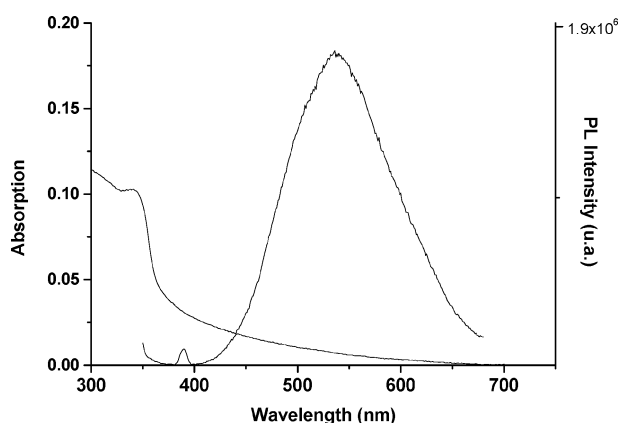


Fig. 6 Absorption and emission spectra of ZnO nanoparticles capped with **1** and APTES used in a 4 : 1 molar ratio.

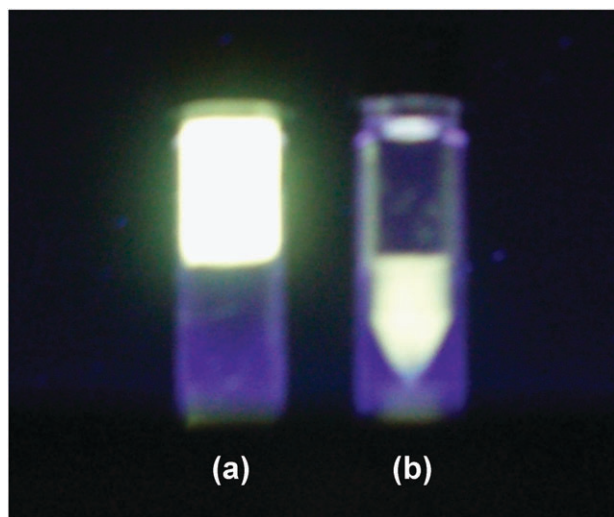


Fig. 7 Photograph of the ZnO QDs excited by an ultraviolet lamp in a biphasic toluene/water mixture (a) before and (b) after ligand exchange.

where E_g^{bulk} is the bulk energy gap, r is the particle radius, m_e is the effective mass of the electrons, m_h is the effective mass of the holes, \hbar is the Planck's constant divided by 2π , and e is the charge of the electron ($m_e = 0.28 m_0$ and $m_h = 0.59 m_0$ where m_0 is the free electron mass). Using this model and the absorption onset of 345 nm (3.59 eV) (obtained by differentiating the absorption spectra depicted in Fig. 2, 4 and 6), the ZnO particles diameter was estimated to be constant (ca. 5.1 nm) before and after ligand exchange. These values are in good agreement with the average diameters determined from the AFM data previously described since particles diameters resulting from AFM measurements appear to be a little larger, which is ascribed to the measurements errors of the contact mode.

Conclusions

In summary, biocompatible ZnO nanoparticles were synthesized from oleate-capped ZnO nanoparticles through surface functionalization with PEG-siloxane **1**. The PEG groups at the

outer surface of the nanocrystal–ligand complex render excellent water solubility for the dots after the siloxane unit bonded to the OH groups on the surface of the ZnO QDs. Using AFM and UV-Vis spectroscopy, we demonstrated that the diameters of the QDs did not significantly change during the ligand exchange. Although moderate quantum yields were obtained after functionalization, the siloxane coating did not quench the PL of the ZnO QDs. Using the PEG-siloxane capping procedure, ZnO nanocrystals without any heavy metal ions can be made to be efficient, stable, small and water soluble, and are potential fluorescent labels for biological systems.

Acknowledgements

This work was supported by the research funds of the French “Ligue Nationale Contre le Cancer, Comités Lorrains”. The authors thank Dr Manuel Dossot (LCPME, UMR CNRS-UHP 7564) for his valuable comments and Olivier Soppera (UMR CNRS 7525) for acquiring the AFM images.

References

1. X. Michalet, F. F. Pinaud, L. A. Bentolila, J. M. Tsay, S. Doose, J. J. Li, G. Sundaresan and A. M. Wu, *Science*, 2005, **307**, 538.
2. R. Robelek, L. F. Niu, E. L. Schmid and W. Knoll, *Anal. Chem.*, 2004, **76**, 6160.
3. W. E. Doering and S. M. Nie, *J. Phys. Chem. B*, 2002, **106**, 311.
4. X. H. Gao, Y. Y. Cui, R. M. Levenson, L. W. K. Chung and S. M. Nie, *Nat. Biotechnol.*, 2004, **22**, 969.
5. W. J. Parak, T. Pellegrino and C. Plank, *Nanotechnology*, 2005, **16**, R9.
6. X. Michalet, F. Pinaud, T. D. Lacoste, M. Dahan, M. P. Bruchez, A. P. Alivisatos and S. Weiss, *Single Mol.*, 2001, **2**, 261.
7. X. Chu, D. Jiang, A. B. Djuricic and H. L. Yu, *Chem. Phys. Lett.*, 2005, **401**, 426.
8. J. C. Johnson, H. Q. Yan, R. D. Schaller, L. H. Haber, R. J. Saykally and P. D. Yang, *J. Phys. Chem. B*, 2001, **105**, 11387.
9. O. G. Schmidt and K. Eberl, *Nature*, 2001, **410**, 168.
10. K. Keis, L. Vayssieres, S.-E. Lindquist and A. Hagfeldt, *Nanostruct. Mater.*, 1999, **12**, 487.
11. Y. L. Wu, C. S. Lim, S. Fu, A. I. Y. Tok, H. M. Lau, F. Y. C. Boey and X. T. Zeng, *Nanotechnology*, 2007, **18**, 215614.
12. A. M. Derfus, W. C. W. Chen and S. N. Bhatia, *Nano Lett.*, 2004, **4**, 11.
13. K. M. Reddy, K. Feris, J. Bell, D. G. Wingett, C. Hanley and A. Punnoose, *Appl. Phys. Lett.*, 2007, **90**, 213902.
14. D.-P. Liu, G.-D. Li, Y. Su and J.-S. Chen, *Angew. Chem., Int. Ed.*, 2006, **45**, 7370.
15. N. S. Norberg and D. R. Gamelin, *J. Phys. Chem. B*, 2005, **109**, 20810.
16. M. A. Garcia, J. M. Merino, E. Fernandez Pinel, A. Quesada, J. De la Venta, M. L. Ruiz Gonzales, G. R. Castro, P. Crespo, J. Liopis, J. M. Gonzales-Calbet and A. Hernando, *Nano Lett.*, 2007, **7**, 1489.
17. Y. L. Wu, A. I. Y. Tok, F. Y. C. Boey, X. T. Zeng and X. H. Zhang, *Appl. Surf. Sci.*, 2007, **253**, 5473.
18. M. Li, H. Bala, X. Lv, X. Ma, F. Sun, L. Tang and Z. Wang, *Mater. Lett.*, 2007, **61**, 690.
19. H.-M. Xiong, D.-P. Liu, Y.-Y. Xia and J.-S. Chen, *Chem. Mater.*, 2005, **17**, 3062.
20. H.-M. Xiong, Z.-D. Wang, D.-P. Liu, J.-S. Chen, Y.-G. Wang and Y.-Y. Xia, *Adv. Funct. Mater.*, 2005, **15**, 1751.
21. C.-H. Hung and W.-T. Whang, *J. Mater. Chem.*, 2005, **15**, 267.
22. N. R. Jana, H. H. Yu, E. M. Ali, Y. Zheng and J. Y. Ying, *Chem. Commun.*, 2007, 1406.
23. H.-M. Xiong, D. P. Xie, X.-Y. Guan, Y.-J. Tan and Y.-Y. Xia, *J. Mater. Chem.*, 2007, **17**, 2490.

24. A. B. Bourlinos, A. Stassinopoulos, D. Anglos, R. Herrera, S. H. Anastasiadis, D. Petridis and E. P. Giannelis, *Small*, 2006, **2**, 513.
25. R. De Palma, S. Peeters, M. J. Van Bael, H. Van den Rul, K. Bonroy, W. Laureyn, J. Mullens, G. Borghs and G. Maes, *Chem. Mater.*, 2007, **19**, 1821.
26. Q. Yang, S. Ma, J. Li, F. Xiao and H. Xiong, *Chem. Commun.*, 2006, 2495.
27. W. R. Dawson and M. W. Windsor, *J. Phys. Chem.*, 1968, **72**, 3251.
28. Q. Wan and T. H. Wang, *Appl. Phys. Lett.*, 2005, **87**, 083–105.
29. F. Q. He and Y. P. Zhao, *Appl. Phys. Lett.*, 2006, **88**, 193–113.
30. K. Vanheusden, W. L. Warren, C. H. Seager, D. R. Tallant, J. A. Voigt and B. E. Gnade, *J. Appl. Phys.*, 1996, **79**, 7983.
31. H. Zhou, H. Alves, D. M. Hofmann, B. K. Meyer, G. Kaczmarczyk, A. Hoffmann and C. Thomsen, *Phys. Status Solidi B*, 2002, **229**, 825.
32. W. Z. Ostwald, *Phys. Chem.*, 1901, **37**, 385.
33. L. Brus, *J. Phys. Chem.*, 1986, **90**, 2555.